

A broadband dielectric spectroscopy study of the relaxation behaviour of subsoil

Norman Wagner, Klaus Kupfer and Eberhard Trinks
Institute of Material Research and Testing, Weimar, Coudraystr. 9, 99423 Weimar

ABSTRACT: The complex dielectric permittivity or electrical conductivity of saturated and unsaturated soils was examined in the frequency range from 1 MHz up to 20 GHz at room temperature and under atmospheric pressure. Three soil-specific relaxation processes are assumed to act in the investigated frequency-temperature-pressure range. The dielectric relaxation behaviour is parameterised with the use of a simple fractional relaxation model as a function of moisture. The chosen approach provide an estimate of the frequency depended dielectric permittivity based on a parameterisation of each relaxation processes as a function of water content and porosity.

Keywords: dielectric spectroscopy, subsoil, lossy dielectrics, fractional relaxation

1 Introduction

High frequency electromagnetic determination of moisture in porous media, e.g. soil, is based on the strong relationship between volumetric water content and relative dielectric permittivity. However, various factors affect this relationship such as measurement frequency, temperature, mineralogical composition, structure, texture, bulk density and chemical composition of the pore fluid [1, 2, 4, 6, 8, 16, 22, 24]. In particular, knowledge of the spatial and temporal variability of water saturation in soils is important to obtain improved estimates of water flow through structures of flood protecting and subsurface disposal as well as the vadose zone [7, 8, 11, 17, 22]. Therefore, the objective of numerous experimental, numerical and theoretical investigations is the development of general calibration rules for a broad class of soil textures and structures [1, 21, 22, 24, 25, 27, 23, 26].

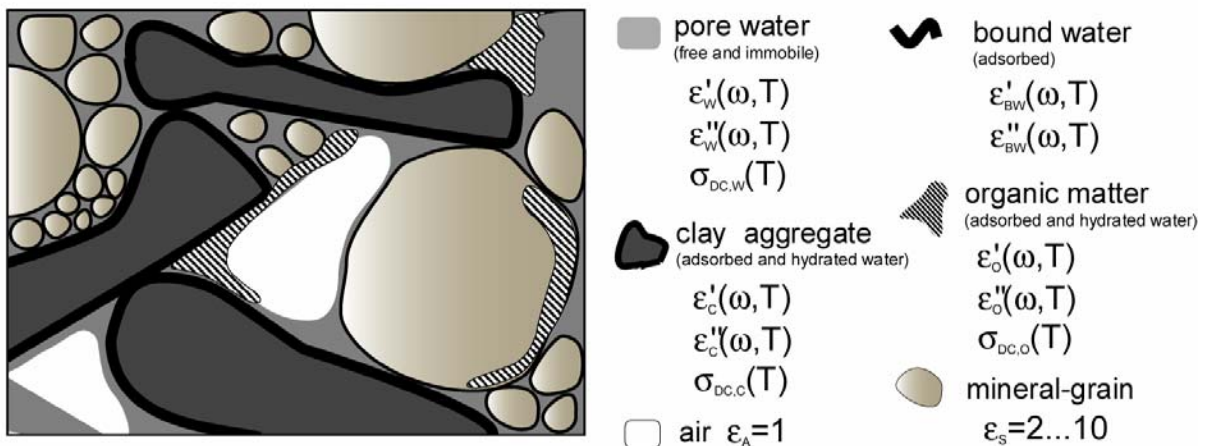


Figure 1: Simplified schematic illustration of unsaturated soil structure with the contribution to the dielectric properties due to several relaxation processes.

Mostly these models are based on the assumption of a constant dielectric permittivity in a narrow frequency range around 1GHz as a function of volumetric water content [10, 21, 25]. However, the strong frequency dependence in the dielectric relaxation behaviour below 1 GHz due to a certain amount of clay minerals in nearly each real soil is considered only insufficiently [16, 18, 29]. The type of multi-scale structure renders the analysis of dynamic data in soils rather complex (c.f. Fig.1). The problem has been addressed both by experimental and modelling techniques [4, 12, 18, 19, 20]. Previous results suggest that clay-

water systems have multiple relaxation processes, such as interfacial polarizations around the clay particles and rotational relaxation of bound and free water, therefore, the dielectric behaviour is expect to be complicated and poor understood [9, 12, 20]. Useful and precise dielectric information may be obtained only when each relaxation process is extracted from the complicated overall behaviour based on the measurement over as wide as possible frequency and temperature ranges and at high resolutions [12].

2 Dielectric relaxation behaviour of moist soil

Based on Maxwell's equations of electrodynamics, an effective current density $\vec{J}_E = \vec{J}_C + \vec{J}_D$ is separated in a conduction current density $\vec{J}_C = \sigma \vec{E}$ (Ohm's Law) and a displacement current density $\vec{J}_D = \epsilon_0 \epsilon_r \partial \vec{E} / \partial t$ with electrical conductivity σ , absolute permittivity of free space ϵ_0 and relative dielectric permittivity ϵ_r . Considering a time varying electrical field strength $\vec{E} = \vec{E}_0 \exp(-j\omega t)$ with angular frequency $\omega = 2\pi f$ this leads to

$$\vec{J}_C(\omega) = \sigma \vec{E}(\omega), \quad \vec{J}_D(\omega) = -j\omega \epsilon_0 \epsilon_r \vec{E}(\omega) \quad (1)$$

The ratio of the absolute values of (1) is defined as the loss factor $\tan \delta$

$$\tan \delta = \frac{|\vec{J}_C(\omega)|}{|\vec{J}_D(\omega)|} = \frac{\sigma}{\omega \epsilon_0 \epsilon_r} \quad (2)$$

The critical frequency $f_c = \omega_c (2\pi)^{-1}$ is given by $\tan \delta = 1$. In the low frequency range $f \ll f_c$, $\tan \delta$ becomes $\gg 1$, and \vec{J}_D is negligible against \vec{J}_C . This condition defines the boundary between steady and quasi-steady state and wave phenomena. The material acts in this case as a conductor. For the case $\tan \delta \ll 1$ at which \vec{J}_C is negligible against \vec{J}_D , the material acts as an insulator (see Fig. 2, [15]).

Under these circumstances the broadband electromagnetic transfer functions $\tilde{\epsilon}_{\text{eff}}(\omega)$ or $\tilde{\sigma}_{\text{eff}}(\omega)$ of a soil sample can be characterise by the dependence of the absolute complex dielectric permittivity $\tilde{\epsilon}(\omega) = \epsilon_0 \tilde{\epsilon}_r(\omega) = \epsilon'(\omega) - j\epsilon''(\omega)$ and the complex electrical conductivity $\tilde{\sigma}(\omega) = \sigma'(\omega) + j\sigma''(\omega)$ on frequency f as well as on thermodynamic state parameters like temperature, pressure and water content [3, 13]. Then under consideration of (1) the effective current density $\vec{J}_E(\omega)$ becomes:

$$\vec{J}_E(\omega) = \tilde{\sigma}_{\text{eff}}(\omega) \vec{E}(\omega) = \tilde{\epsilon}_{\text{eff}}(\omega) \frac{\partial \vec{E}(\omega)}{\partial t}, \quad \tilde{\sigma}_{\text{eff}}(\omega) = j\omega \tilde{\epsilon}_{\text{eff}}(\omega) \quad (3)$$

with

$$\tilde{\epsilon}_{\text{eff}}(\omega) = \epsilon_0 \epsilon'_r(\omega) + \frac{\sigma''(\omega)}{\omega} - j \left(\epsilon_0 \epsilon''_r(\omega) + \frac{\sigma'(\omega)}{\omega} \right) = \epsilon'_{\text{eff}}(\omega) - j\epsilon''_{\text{eff}}(\omega) \quad (4)$$

$$\tilde{\sigma}_{\text{eff}}(\omega) = \sigma'(\omega) + \omega \epsilon_0 \epsilon''_r(\omega) + j(\sigma''(\omega) + \omega \epsilon_0 \epsilon'_r(\omega)) = \sigma'_{\text{eff}}(\omega) + j\sigma''_{\text{eff}}(\omega) \quad (5)$$

From these relations follows that the real part of $\tilde{\sigma}_{\text{eff}}$ acts as an ohmic conductance and therefore σ' and ϵ''_r are linked to a movement of charges. Otherwise the real part of $\tilde{\epsilon}_{\text{eff}}$ acts as a capacitive susceptance and a charge displacement is linked to ϵ'_r and σ'' . Based on these circumstances it is reasonable to define a real effective relative permittivity $\epsilon_{r,\text{eff}}$ and a real effective conductivity σ_{eff} (c.f. Fig. 2):

$$\epsilon_{r,\text{eff}}(\omega) = \frac{\epsilon'_{\text{eff}}(\omega)}{\epsilon_0} = \epsilon'_r(\omega) + \frac{\sigma''(\omega)}{\epsilon_0\omega}, \quad (6)$$

$$\sigma_{\text{eff}}(\omega) = \sigma'_{\text{eff}}(\omega) = \sigma'(\omega) + \omega\epsilon_0\epsilon''_r(\omega) \quad (7)$$

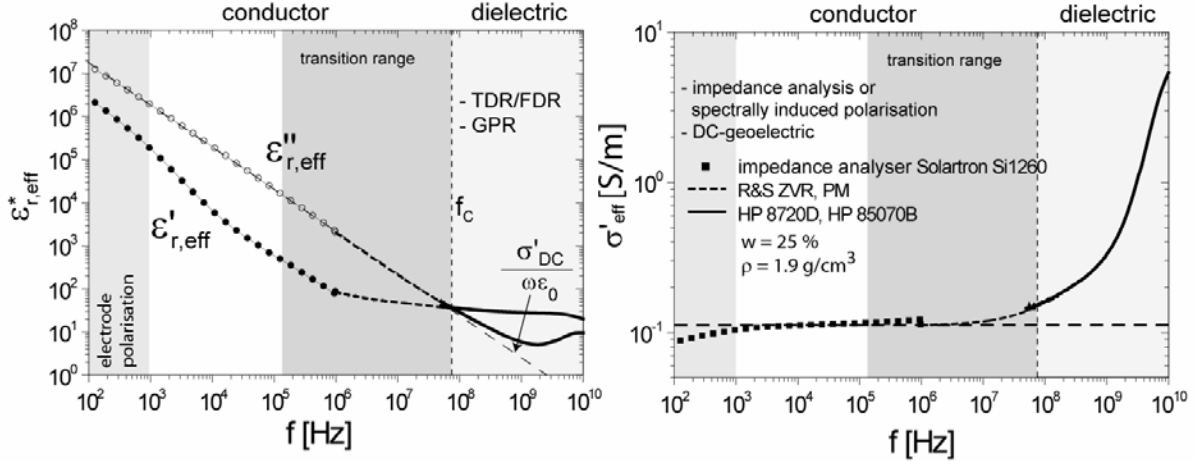


Figure 2: Relative complex dielectric permittivity $\tilde{\epsilon}_{r,\text{eff}}$ and real part of the complex electrical conductivity $\tilde{\sigma}_{\text{eff}}$ of the silty clay loam sample (dike at river Unstrut/germany).

The critical frequency f_c is perhaps the most important parameter when considering the electrical mechanisms of moist soil. Especially in time domain reflectometry (TDR) applications with flat bad cable sensors the effective sensor length is restricted by f_c [17]. At frequencies above f_c , $\epsilon_{r,\text{eff}}(\omega)$ is the most effective parameter, which determines the general dielectric relaxation characteristics of soil. Below f_c , $\sigma_{\text{eff}}(\omega)$ is the most effective parameter and common mixing models fail ([15]). In order to analyse the frequency range that includes more than 12 orders (1MHz - 3GHz) of frequency, a simple broad band transfer function is suggested by Börner [3] (Combined Conductivity and Permittivity Model - CCPM) for moist rocks:

$$\tilde{\epsilon}_{\text{eff}}(\omega) = \epsilon_0\epsilon_\infty + \epsilon_0\epsilon_{r,1}(j\omega\tau)^{n-1} - j\omega^{-1}(\sigma_{\text{DC}} + \sigma_1(j\omega\tau)^{1-p}) \quad (8)$$

with high frequency limit of permittivity ϵ_∞ , angular frequency ω , direct current electrical conductivity σ_{DC} , a frequency independent conductivity σ_1 as well as relative dielectric permittivity $\epsilon_{r,1}$, relaxation time τ and stretching exponents $0 \leq p, n \leq 1$. The frequency dependence of relative permittivity and conductivity of subsoil can be calculated with this model in the frequency range up to ~1GHz. However, the relaxation behaviour can not be described completely in the frequency range above 1 GHz. For this purpose in comparison to (8) the dielectric relaxation behaviour of each expected process is described by a fractional relaxation model according to Wagner et al. [28]. In order to parameterise the measured spectra as a function of water content w and bulk density ρ a generalized dielectric response (GDR) was used under assumption of three relaxation processes:

$$\tilde{\epsilon}_{\text{eff}}(\omega) - \epsilon_\infty = \sum_{i=1}^3 \frac{\Delta\epsilon_i}{(j\omega\tau_i)^{\alpha_i} + (j\omega\tau_i)^{\beta_i}} - j \frac{\sigma_{\text{DC}}}{\omega\epsilon_0} \quad (9)$$

with relaxation strength $\Delta\varepsilon_i$, relaxation time τ_i and stretching exponents $0 \leq \alpha_i, \beta_i$ of the i -th process.

3 Experiments

The complex dielectric permittivity of saturated and unsaturated soil was examined in the frequency range 1 MHz to 20 GHz at room temperature and under atmospheric pressure with a Rohde & Schwarz ZVR (1 MHz - 4 GHz), with a PNA E8363B (10 MHz - 40 GHz) and with a HP8720D (50 MHz to 20 GHz) network analyser. This was performed using a combination of open-ended coaxial-line (HP85070B) and coaxial transmission line technique (sample holder $(7 \times 16 \times 100) \text{mm}^3$) ([29]). In addition, selected soil-samples were examined in the frequency range 1 Hz - 1 MHz with a Solartron Si 1260 - impedance analyser (see Fig. 2).

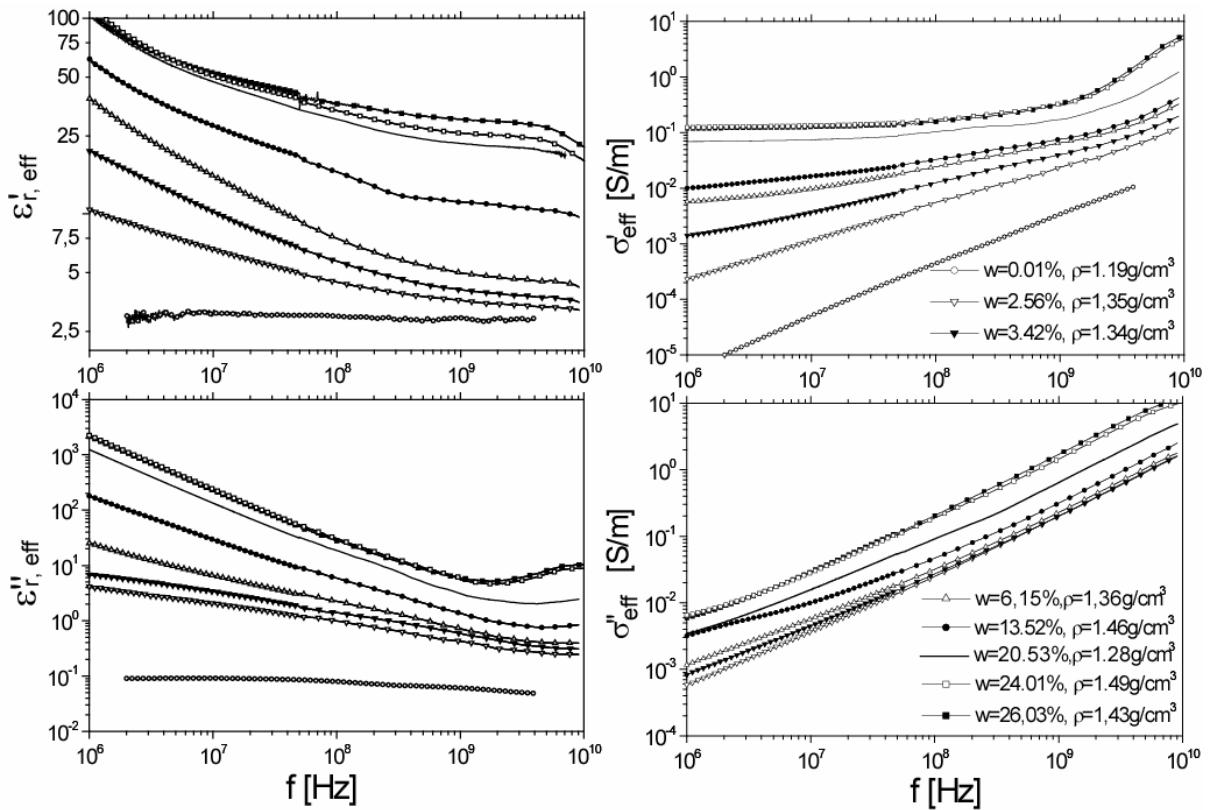


Figure 3: Complex effective relative dielectric permittivity $\tilde{\varepsilon}_{r,\text{eff}}$ and complex effective electrical conductivity $\tilde{\sigma}$ as a function of frequency of the silty clay loam sample for selected gravimetric water contents w and dry bulk densities ρ .

Fig. 3 represents our results of a silty clay loam from a dike at the river Unstrut, Thuringia, Germany: 29.7% clay, 49.8% silt, 19.9% sand and an effective cation exchange capacity $\text{CEC} = 65.6 \text{ mmol}(\text{eq})/100\text{g}$. The samples were selected from a larger data set of up to 40 measurements representative for the investigated broad frequency range and a narrow porosity range (see Tab. 1). The soil samples were incrementally wetted from air dry up to saturation with natural water and equilibrated 12h. From the prepared sample a subsample was taken. A retaining ring was used as the sample holder for the HP85070B probe. Care was taken to pack the soil in the transmission line to a homogeneous bulk density and to a defined volume. After each dielectric measurement bulk density ρ as well as gravimetric water content w were determined. The complex permittivity was calculated in the frequency range 50 MHz to 8 or 20 GHz with the HP 85070/71C Materials Measurement Software. In addition the

measured complex S-parameter values were used to compute $\epsilon_{r,\text{eff}}(\omega)$ in the frequency range 1 MHz to 4 GHz after full to port calibration of the coaxial transmission line with different methods: Nicolson-Ross-Weir technique and propagation matrix method [5].

4 Discussion

Three relaxation processes are assumed to act in the investigated frequency-temperature-pressure range: one primary α -process (main water relaxation) and two secondary (α',β)-processes due to clay-water-ion interactions (bound water relaxation and the Maxwell-Wagner effect respectively). A Shuffled Complex Evolution Metropolis (SCEM-UA) algorithm ([8]) is used to find best GDR or CCPM fitting parameters (Tab. 1, Fig. 3). This algorithm is an adaptive evolutionary Monte Carlo Markov Chain method and combines the strengths of the Metropolis algorithm, controlled random search, competitive evolution, and complex shuffling ([8]) to obtain an efficient estimate of the most optimal parameter set, and its underlying posterior distribution, within a single optimisation run. The resulting relative error of each parameter is less than 3%.

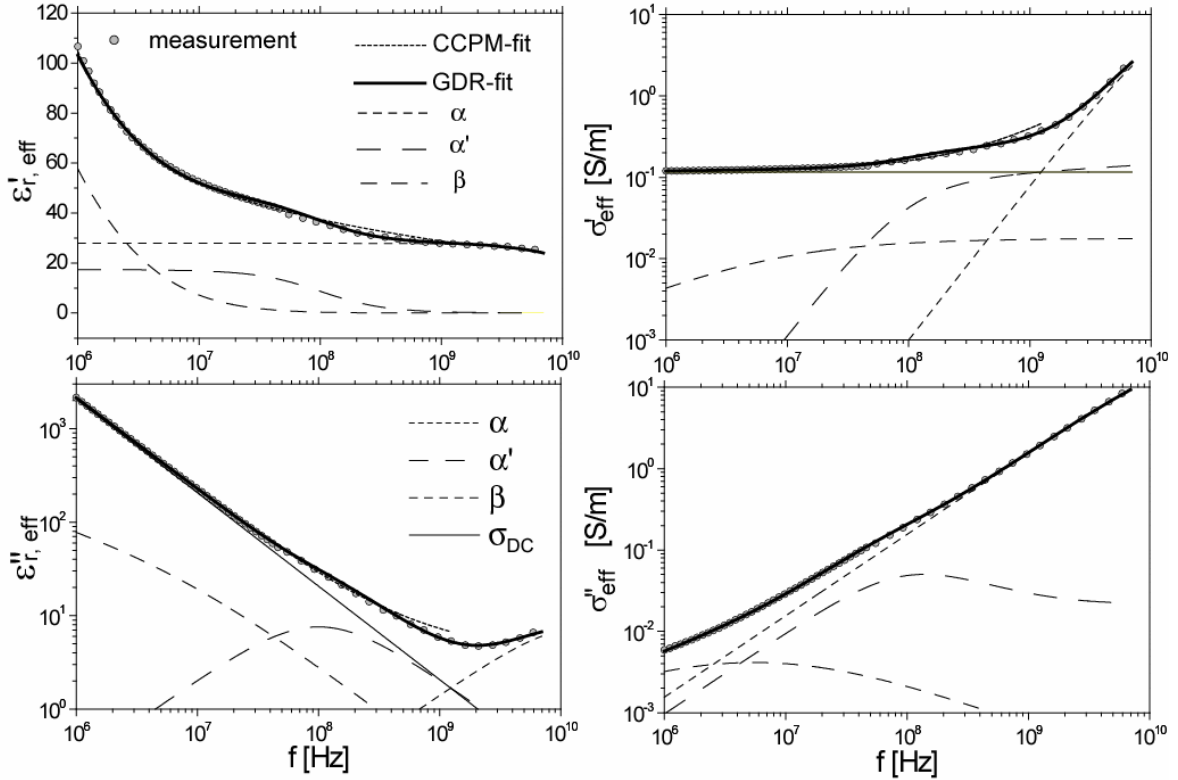


Figure 3: Complex relative dielectric permittivity $\tilde{\epsilon}_r$ and conductivity $\tilde{\sigma}$ as a function of frequency of the sample v-10 with the result of the SCEM-UA optimisation (Tab. 1).

Beside the data obtained in the SCEM-UA optimisation, the relative dielectric permittivity at a measurement frequency of 1 GHz, $\epsilon_{r,1\text{GHz}}$ and the critical frequency f_c according to (2) for the spectra in Fig. 3 are summarised in Tab. 1. Relative dielectric permittivity $\epsilon_{r,1\text{GHz}}$ follows Topp's calibration function [26]: $\epsilon_r = 3.03 + 9.39 + 1469^2 - 76.79^3$. f_c increases to a maximum value of 127 MHz at a volumetric water content of $\vartheta = 19.71\%$ with increasing water content and then decreases to 70 MHz at $\vartheta = 37.33\%$. The relaxation parameters obtained from GDR-fit are presented in Tab. 1 and Fig. 4. Relaxation strength $\Delta\epsilon_i$ of each process as well as apparent direct current electrical conductivity σ_{DC} and the stretch exponents α_i depend strongly on moisture content.

Table 1: Parameters determined in the SCEM-UA optimisation with GDR as well as CCPM; gravimetric water content w , dry bulk density ρ , porosity ϕ and volumetric water content ϑ of the selected silty clay loam samples.

	v-1	v-2	v-3	v-4	v-5	v-6	v-7	v-8	v-9	v-10
w [%]	2.56	3.42	3.71	6.15	8.95	14.00	13.52	20.53	24.01	26.03
ρ [g/cm ³]	1.35	1.34	1.33	1.36	1.27	1.11	1.46	1.27	1.49	1.43
ϕ	0.50	0.50	0.50	0.49	0.53	0.57	0.46	0.51	0.45	0.47
ϑ [%]	3.47	4.57	4.95	8.37	11.34	15.61	19.71	26.05	35.74	37.33
f_c [MHz]	<1	<1	1.5	13.59	34.34	46.7	127.3	69.9	83.23	70.0
$\epsilon_{1\text{GHz}}$	3.47	3.70	4.11	4.62	5.69	6.27	10.64	14.86	25.22	25.49
GDR-Parameter										
ϵ_∞	1.38	0.93	0.82	2.28	2.50	2.60	3.18	3.96	1.92	2.29
$\Delta\epsilon_\alpha$	1.95	2.09	2.64	2.06	2.29	3.01	6.98	9.83	21.97	24.31
τ_α [ps]	0.31	0.25	0.59	3.11	4.91	5.113	4.91	8.83	5.08	5.90
α_α (fixed)	0.00	0.00	0.00	0.00	0.00	0.00	0.00	0.00	0.00	0.00
$1-\beta_\alpha$	0.49	0.30	0.19	0.08	0.03	0.00	0.04	0.09	0.02	0.05
$\Delta\epsilon_{\alpha'}$	5.25	7.76	9.74	15.81	14.60	14.39	20.38	25.16	23.70	22.06
$\tau_{\alpha'}$ [ns]	9.89	9.86	9.69	9.97	9.94	9.40	4.52	9.46	2.28	2.12
$\alpha_{\alpha'}$ (fixed)	0.00	0.00	0.00	0.00	0.00	0.00	0.00	0.00	0.00	0.00
$1-\beta_{\alpha'}$	0.44	0.47	0.44	0.38	0.43	0.40	0.36	0.39	0.33	0.26
$\Delta\epsilon_\beta$	3.61	6.46	10.10	48.33	56.79	44.93	58.94	105.18	164.49	83.90
τ_β [ns]	63.32	49.47	37.38	67.46	28.47	36.79	56.21	92.81	52.95	36.60
α_β (fixed)	1.00	1.00	1.00	1.00	1.00	1.00	1.00	1.00	1.00	1.00
$1-\beta_\beta$	0.74	0.74	0.65	0.46	0.40	0.37	0.50	0.41	0.36	0.40
σ_{DC} [S/m]	5.3E-5	6.26-5	7.8E-4	3.0E-3	4.0E-3	0.01	0.07	0.048	0.11	0.11
CCPM-Parameter										
ϵ_∞	2.36	2.01	2.74	2.83	2.16	4.24	3.89	4.01	4.93	1.38
ϵ_1	1.14	0.27	0.02	3.19	3.35	2.74	9.12	11.95	28.84	29.26
τ_1 [ns]	173.1	496.5	429.9	411.4	0.9	0.96	0.2	0.64	2.0	0.3
n	0.84	1.00	0.86	0.84	0.92	0.82	0.77	0.91	0.89	0.88
σ_{DC} [S/m]	3.0E-06	7.1E-09	0.001	0.004	0.005	0.001	0.023	0,027	0.116	0.061
σ_1 [S/m]	9.1E-04	4.7E-04	0.001	0.003	0.003	0.007	0.044	0,020	0.010	0.056
τ_2 [ns]	56.3	355.8	261.9	133.6	849.0	892.16	988.2	283,42	161.6	783.7
p	0.31	0.34	0.39	0.47	0.65	0.78	0.99	0,83	0.77	0.97

Relative high frequency permittivity ϵ_∞ determined in the SCEM-UA optimisation with GDR (2.2 ± 1) as well as CCPM (3.16 ± 1.2) varies within a small range. Relaxation time of main water relaxation τ_α is lower than the expected relaxation time of pure water at 20°C and under atmospheric pressure with $\tau_{\text{water}} = 9.37$ ps ([14]). However, τ_α slightly increases with increasing volumetric water content to $\tau_\alpha = 5.9$ ps. Relaxation time $\tau_{\alpha'}$, which is referred to as bound water, decreases with increasing volumetric water content from 9.9 ns to 2.12 ns. The current understanding of bound water relaxation suggests that the closer the water layer is to the particle the more distorted is its structure compared to the structure of free water τ_w or ice

τ_i , with $\tau_w < \tau_{bw} < \tau_i$ [2]. Hilhorst et al. [9] conclude based on literature data a bound water relaxation time $\tau_{bw} > 16$ ns. In contrast Boyarskii et al. [2] suggest a decrease of the mean relaxation time of bound water from ~ 0.5 ns to 7.7 ps at 27°C due to an increasing number of molecular water layers with increasing volumetric water content.

The determined relaxation time τ_β is referred to as relaxation mechanism involving strong clay–water-ion interactions, e.g. the Maxwell–Wagner effect. In the investigated frequency–temperature–pressure range τ_β shows no systematic dependence on moisture. Ishida et al. [12] reported a relaxation time at about 160 ns in clay suspensions using TDR. In addition, Dudley et al. [4] found relaxation times based on impedance spectroscopy measurements of about 22 ns for Na-montmorillonite and 160 ns for Ca-montmorillonite suspensions. The obtained values from GDR-fit $\tau_\beta = (51 \pm 19)$ ns are within this range.

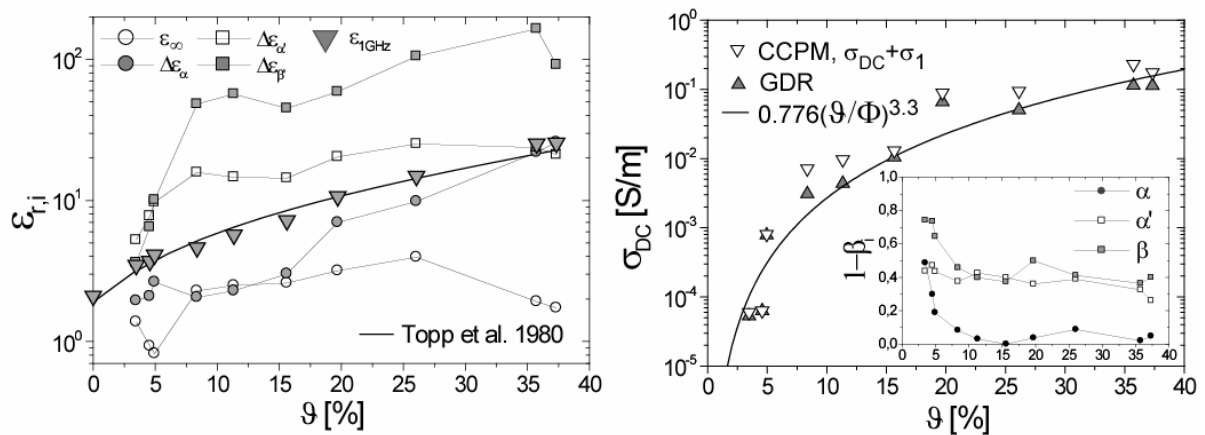


Figure 4: (left) Relaxation strength $\Delta\epsilon_i$ of the i -th process in comparison to the relative high frequency permittivity ϵ_∞ , (right) apparent direct current electrical conductivity σ_{DC} and (inset) distribution parameter of the i -th process as a function volumetric water content θ .

5 Conclusion

The results show the potential of the chosen approach but a detailed explanation of this complex behaviour is beyond the scope of this paper. In general, there is a need of further systematic investigations by broadband dielectric spectroscopy of saturated and unsaturated soils under controlled hydraulic and mechanical conditions and with an utilisation of microscopic modelling.

Acknowledgement

The authors grateful acknowledge the project agency for Water Technology and Waste Management of the BMBF for support of the project 02WH0487.

References

- [1] Behari, J. (2005) Microwave Dielectric Behaviour of Wet Soils. Springer
- [2] Boyarskii, D. A., Tikhonov, V. V. and Komarova N. Yu. (2002) Model of dielectric constant of bound water in soil Progress In Electromagnetics Research, PIER 35, 251–269
- [3] Börner, F. (2006) Complex Conductivity Measurements. in Kirsch, R. (Ed.): Groundwater Geophysics, Springer, 119-153
- [4] Dudley, L.M., Bialkowski, S., Or, D., Junkermeier, C. (2003) Low frequency impedance behavior of montmorillonite suspensions: Polarization mechanisms in the low frequency domain. Soil Sci. Soc. Am. J. 67: 518 – 526.

- [5] Gorriti, A.G. (2004) Electric characterization of sands with heterogeneous saturation distribution, PhD Thesis, Technical University Delft
- [6] Fechner, T., Börner, F., Richter, T., Yaramancy, U. and Wehnacht B. (2004) Lithological Interpretation of the Spectral Dielectric Properties of Limestone. *Near Surface Geophysics*, 23:150-159
- [7] Gutina, A., Antropova, T., Rysiakiewicz-Pasek, E., Virnik, K. and Feldman, Yu. (2003) Dielectric relaxation in porous glasses, *Microporous and Mesoporous Materials*, Vol. 58, (3), 2003, 237-254.
- [8] Heimovaara, T. J., Huisman, J. A., Vrugt, J. A., Bouten, W. (2004) Obtaining the spatial distribution of water content along a TDR probe using the SCEM-UA bayesian inverse modelling scheme. *Vadose Zone J.* 3:1128–45
- [9] Hilhorst, M.A., Dirksen, C., Kampers, F.W.H., Feddes, R.A. (2001) Dielectric Relaxation of Bound Water versus Soil Matric Pressure. *Soil Sci Soc Am J* 2001 65: 311-314
- [10] Hoekstra, P., Delaney, A. (1974) Dielectric properties of soils at UHF and microwave frequencies, *Journal of Geophysical Research*, 79, 11:1699-1708
- [11] Hanafy, S. and al Hagrey, S. A. (2006) Ground-penetrating radar tomography for soil-moisture heterogeneity. *Geophysics*, 71(1):K9-K18, 2006.
- [12] Ishida, T., Makino, T. and Wang, C. (2000) Dielectric-relaxation spectroscopy of kaolinite, montmorillonite, allophane, and imogolite under moist conditions. *Clays Clay Miner.* 48:75–84
- [13] Jonscher, A. K. (1977), *Nature*, 267, 673-679
- [14] Kaatze, U. (2005) Electromagnetic Wave Interactions with Water and Aqueous Solutions, In K. Kupfer (Ed.), *Electromagnetic Aquametry*, (2005) Springer, 15-37
- [15] Katsube, T.J., Collet L.S. in Strens, R. G. J.: *The Physics and Chemistry of Minerals and Rocks*. John Wiley & Sons, London (1974), 279-295
- [16] Kelleners, T. J., Robinson, D. A., Shouse, P. J., Ayars, J. E., Skaggs, T. H. (2005) Frequency dependence of the complex permittivity and its impact on dielectric sensor calibration, *Soil. Sci. Soc. Am. J.*, 69, 67-76
- [17] Kupfer, K., Trinks, E. (2005) Simulations and experiments for detection of moisture profiles with TDR in a saline environment, In K. Kupfer (Ed.), *Electromagnetic Aquametry*, (2005) Springer, 349-365
- [18] Logsdon, S. D. (2005) Soil Dielectric Spectra from Vector Network Analyzer Data. *Soil Sci Soc Am J*, 69(4):983-989, 2005.
- [19] Logsdon, S. and Laird, D. (2004) Cation and water content effects on dipole rotation activation energy of smectites. *Soil Sci. Soc. Am. J.* 68:1586–91
- [20] Malikova, N., Cadene, A., Marry, V., Dubois, E., Turq, P., Zanotti, J.-M. and Longeville, S. (2005) Diffusion of water in clays, microscopic simulation and neutron scattering. *Chem. Phys.* 317:226–35
- [21] Regalado, C. M. (2006) A geometrical model of bound water permittivity based on weighted averages: the allophone analogue. *J. Hydrol.* 316:98–107
- [22] Robinson, D. A., Jones, S. B., Wraith, J. M., Or, D., Friedman, S. P. (2003), A Review of Advances in Dielectric and Electrical Conductivity Measurement in Soils Using Time Domain Reflectometry, *Vadose Zone J* 2:444-475
- [23] Roth, C.H., Malicki, M.A., Plagge, R. (1992) Empirical evaluation of the relationship between soil dielectric constant and volumetric water content as the basis for calibrating soil moisture measurement by TDR. *J. Soil Sci.* 43:1–13
- [24] Shen, L., Savre, W., Price, J., Athavale, K. (1985) Dielectric properties of reservoir rocks at ultra-high frequencies. *geophysics*, 50(4):629-704, 1985.
- [25] Sihvola, A. (2000) *Electromagnetic Mixing Formulae and Applications*. Number 47 in IEE Electromagnetic Waves Series. INSPEC, Inc, 2000.
- [26] Topp, G. C., Davis, J. L., Annan, A. (1980) Electromagnetic determination of soil water content: Measurement in coaxial transmission lines. *Water Resources Research*, 16(3):574--582, 1980.
- [27] Tuncer, E., Serdyuk, Y. V., Gubanski, S. M. (2001) Dielectric mixtures - electrical properties and modelling. *IEEE Transactions on Dielectrics and Electrical Insulation* 9, 809-828 (2002)
- [28] Wagner, N., Trinks, E., Kupfer, K. (2005) Development of TDR-Sensors for moist materials using HFSS, Sixth International Conference on Electromagnetic Wave Interaction with Water and Moist Substances, Weimar, Germany, May 29 – June 1, 2005, 107-115.
- [29] Wagner, N., Trinks, E., Kupfer, K. (2006) Determination of the spatial TDR-sensor characteristics in strong dispersive subsoil using 3D-FEM frequency domain simulations in combination with microwave dielectric spectroscopy, *Measurement Science and Technology*, in print

Corresponding author: Norman Wagner, Materialforschungs- und -prüfanstalt an der Bauhaus-Universität Weimar, Coudraystraße 9, 99423 Weimar, Phone: +49-3643-564221, Fax: +49-3643-564204, e-mail: norman.wagner@mfpa.de